# Different Dynamics of CD4$^+$ and CD8$^+$ T Cell Responses During and After Acute Lymphocytic Choriomeningitis Virus Infection[1]

**Rob J. De Boer,[2]* Dirk Homann,[†] and Alan S. Perelson[‡]**

**We fit a mathematical model to data characterizing the primary cellular immune response to lymphocytic choriomeningitis virus. The data enumerate the specific CD8$^+$ T cell response to six MHC class I-restricted epitopes and the specific CD4$^+$ T cell responses to two MHC class II-restricted epitopes. The peak of the response occurs around day 8 for CD8$^+$ T cells and around day 9 for CD4$^+$ T cells. By fitting a model to the data, we characterize the kinetic differences between CD4$^+$ and CD8$^+$ T cell responses and among the immunodominant and subdominant responses to the various epitopes. CD8$^+$ T cell responses have faster kinetics in almost every aspect of the response. For CD8$^+$ and CD4$^+$ T cells, the doubling time during the initial expansion phase is 8 and 11 h, respectively. The half-life during the contraction phase following the peak of the response is 41 h and 3 days, respectively. CD4$^+$ responses are even slower because their contraction phase appears to be biphasic, approaching a 35-day half-life 8 days after the peak of the response. The half-life during the memory phase is 500 days for the CD4$^+$ T cell responses and appears to be lifelong for the six CD8$^+$ T cell responses. Comparing the responses between the various epitopes, we find that immunodominant responses have an earlier and/or larger recruitment of precursors cells before the expansion phase and/or have a faster proliferation rate during the expansion phase.** ***The Journal of Immunology,*** **2003, 171: 3928–3935.**

Studies of the immune response during acute viral infections have frequently focused on the rapid and extensive response of antigen-specific CD8$^+$ T cells (1–5). A typical time course of the acute CD8$^+$ T cell response to lymphocytic choriomeningitis virus (LCMV)[3] involves an extensive proliferation phase, a contraction or death phase, during which 95% of Ag-specific cells die, and a long-term memory phase (3, 6). At the peak of the response, most of the activated CD8$^+$ T cell population in the spleen are specific for LCMV (4). The CD8$^+$ T cell population size during the memory phase remains approximately constant and is typically 5% of the peak value (4).

Homann et al. (7) compared acute CD4$^+$ and CD8$^+$ T cell responses to LCMV in C57BL/6 mice. Both CD4$^+$ and CD8$^+$ T cell responses go through the typical three phases of expansion, contraction, and memory. These phases are fairly synchronous, with the peak of the response around day 8 for CD8$^+$ T cells and around day 9 for CD4$^+$ T cells. The major differences between the two types of response are a 20-fold lower expansion in the CD4$^+$ T cell responses and the fact that memory is stable in CD8$^+$ responses and declining in the CD4$^+$ T cell responses (7). The CD4$^+$ T cell contraction phase was divided into several phases with a progressive increase in the half-life of the Ag-specific T cells. Because the measurements are of total numbers of Ag-specific cells per spleen, these changes in the half-lives should at least partly reflect the differentiation of short-lived activated cells into long-lived memory cells. To test this, we collected new data which we then fit to mathematical models that included these two subpopulations and estimated the half-lives of Ag-specific activated and memory cells for both dominant and subdominant CD4$^+$ and CD8$^+$ T cell responses.

Recent data demonstrate that CD8$^+$ T cells undergo considerable clonal expansion after initial exposure to Ag (8–11). Lau et al. (1) found that CD8$^+$ T cell proliferation continues after the virus has been cleared. A relatively short stimulus by Ag, i.e., less than $<$2 h (9), "programs" CD8$^+$ T cells to divide several times in an Ag-independent manner. Similar results have been found for CD4$^+$ T cells (12–14). Although the molecular basis of Ag-independent proliferation during primary immune reactions is at present not known, a simple model where proliferation is switched on and off, independent of the Ag concentration, seems well suited to fit to data like this (15). In the model given below, the "off" switch, or the time of the peak of the T cell response, is an independent parameter reflecting the end of the programmed cell division cascade. We previously used such a mathematical model to describe the BALB/c CD8$^+$ T cell response to the NP118 and gp283 epitopes of LCMV Armstrong (15). In this study, we extend the model with a biphasic contraction phase.

## Materials and Methods

Data were collected as described previously (7). Briefly, C57BL/6 mice were infected i.p. with $10^5$ PFU of LCMV Armstrong. Splenocytes were obtained at various time points after infection and were analyzed for epitope-specific T cells by intracellular cytokine staining after restimulation with specific epitopes. Each data point in Figs. 1, 2, and 4 is the average of three to four mice (except for the data points at day 921 which are based on two mice). Mice were infected at 6–8 wk of age. Both male and female mice were used, and no apparent differences were noted. In

*Theoretical Biology, Utrecht University, Utrecht, The Netherlands; †Department of Neuropharmacology, Division of Virology, The Scripps Research Institute, La Jolla, CA 92037; and ‡Theoretical Division, Los Alamos National Laboratory, Los Alamos, NM 87545.

Received for publication May 6, 2003. Accepted for publication August 4, 2003.

The costs of publication of this article were defrayed in part by the payment of page charges. This article must therefore be hereby marked *advertisement* in accordance with 18 U.S.C. Section 1734 solely to indicate this fact.

[1] Portions of the work were done under the auspices of the U.S. Department of Energy and supported by National Institutes of Health Grants AI28433 and RR06555 (to A.S.P.). D.H. was supported by National Institutes of Health Training Grant AG00080 and Juvenile Diabetes Foundation International Fellowship 3-1999-629.

[2] Address correspondence and reprint requests to Dr. Rob J. De Boer, Theoretical Biology, Utrecht University, Padualaan 8, 3584 CH Utrecht, The Netherlands. E-mail address: R.J.DeBoer@bio.uu.nl.

[3] Abbreviations used in this paper: LCMV, lymphocytic choriomeningitis virus; MNSQ, mean square; pMHC, peptide MHC.



0022-1767/03/$02.00

C57BL/6 mice infected with LCMV WE, the virus persists at very low levels after infection (16). In our C57BL/6 system with LCMV Armstrong, the virus is controlled effectively, and there is no evidence for residual persisting Ag (1, 7, 17).

We fit the data to a simple mathematical model considering "clones" of activated ($A$) and memory ($M$) cells. Activated cells proliferate and die and become memory cells. Memory cells are formed when activated cells adopt the memory phenotype and die at rate $\delta_M$. Because the proliferation of T cells after antigenic stimulation seems "programmed" (8–14), we split the dynamics into distinct phases with maximal proliferation before the peak of the response, at time $T$, and cell death and formation of memory cells after the peak of the response. For $CD4^+$ T cells, Homann et al. (7) describe a multiphasic contraction phase and thus we additionally consider the possibility of having two distinct phases of activated cell death after the peak of the response.

During the expansion phase, i.e., when $t < T$, we assume that there are no memory cells and that activated T cells proliferate according to

$$\frac{dA}{dt} = \rho A, \tag{1}$$

where $\rho$ is the net expansion rate. Following the peak of the response at time $T$, we may allow for two distinct phases, i.e., a rapid contraction phase of length $\Delta$ days, where activated cells die rapidly by apoptosis or activation-induced cell death, at a rate $\alpha$, and a slower phase where activated cells die at their basic turnover rate $\delta_A$. Memory cells can be formed during the entire contraction phase at rate $r$. Thus, during the rapid contraction phase, i.e., when $T < t < T + \Delta$, the activated and memory T cell population dynamics are governed by the following differential equations:

$$\frac{dA}{dt} = -(r + \alpha + \delta_A)A, \tag{2}$$

$$\frac{dM}{dt} = rA - \delta_M M, \tag{3}$$

where $\alpha$ is the parameter representing rapid apoptosis. During the slower part of the contraction phase, i.e., when $t > T + \Delta$, we set $\alpha = 0$. When most of the activated cells have died or have become memory cells, the model naturally enters the so-called memory phase that is characterized by the average life span $1/\delta_M$ of the memory cells. Since the memory cells are partly maintained by cell renewal (6), $1/\delta_M$ is not a true life span, but the average persistence time of the memory population determined by the net result of renewal and death. Using 5-bromo-2-deoxyuridine labeling, we found that 2–3% of the memory cells are cycling (D. Homann, unpublished data).

We fit the data to models having the rapid apoptosis time window $\Delta$ and to models in which we set $\Delta = \alpha = 0$ (the latter corresponds to our original model (15)). In the version of the model with an explicit early apoptosis time window, the death rate of the activated cells is time dependent, with more rapid death just after the peak of the response. In the version with a single death rate for activated cells, we also observe a biphasic contraction of the total T cell population after the peak, because short-lived activated cells are being replaced by long-lived memory cells. Note that in the $\Delta = \alpha = 0$ version of the model, $\delta_A$ represents a death rate of activated cells combining apoptosis and normal turnover (15).

Estimates for precursor frequencies for viral epitopes have recently become available and vary around $1{:}10^5$ naive $CD8^+$ T cells (18, 19). However, in our experiments no data was collected during the earliest phases of the response, and thus we have ignored modeling the onset of the response (i.e., the $T_{on}$ parameter of De Boer et al. (15) is set to 0). Instead, we consider an immune response that starts at time 0 with $A(0)$ activated cells. This is obviously a simplification, lumping the precursor frequency and the recruitment rate (or recruitment time) into a single parameter. Because our first data point only gives the number of Ag-specific cells at day 4, we cannot distinguish between the precursor frequency at day 0 and the recruitment rate (or recruitment time) during the first few days. We therefore interpret the $A(0)$ parameter as a generalized recruitment parameter. The larger $A(0)$, the larger the presumed precursor frequency and/or the earlier and the better the precursor cells were triggered by Ag.

Since the model is linear in each phase of the response, one can obtain the solutions of the differential equations (see *Appendix*). Parameter estimates were obtained using the DNLS1 subroutine from the Common Los Alamos Software Library, which is based on the Levenberg-Marquardt algorithm (20) for solving nonlinear least-squares problems. These parameters were used to calculate the predicted T cell population size. Ninety-five percent confidence intervals for the inferred parameters were then determined using a bootstrap method (21), where the residuals to the optimal fit were resampled 500 times. The 95% confidence intervals give the range of parameter values that would be accepted at a 5% significance level.

The different models that we consider could all fit the data reasonably well. To compare the quality of the fit of different models, we report the residual mean square (MNSQ), which is the residual sum of squares divided by the residual degrees of freedom, i.e., the difference between the number of data points and the number of free parameters (22). Thus, adding a redundant parameter to a model should increase the residual MNSQ. Additionally, we perform the partial $F$ test to compare two nested models by the difference between their residual sum of squares per additional parameter divided by the residual MNSQ of the largest of the two models (22). The $F$ value delivered by this test can be looked up in statistical tables giving the $F$ value above which the $F$ distribution exceeds a critical percentage. The $F$ distribution is parameterized by 2 df. The one in the numerator is the difference in the number of parameters between the two models. The one in the denominator is the number of degrees of freedom of the largest model (i.e., the number of data points minus the number of parameters). Throughout this article we will accept the hypothesis that the model with the largest number of parameters provides the best fit when the $F$ value exceeds a significance level of $p < 0.05$.

## Results

### *$CD4^+$ T cells*

The measured $CD4^+$ T cell responses to the epitopes gp61 and NP309 are shown in Fig. 1 along with the best fits of the model to the data. The best-fit parameter estimates are given in Table I. The fits appear to agree well with the data. The model with a biphasic decline fits the data significantly better than the model where we enforce a monophasic decline by setting $\Delta = 0$, as illustrated by comparing the panels at the *bottom* of Fig. 1 (biphasic decline) with those at the top (monophasic decline). With the biphasic model, we obtain a better fit between weeks 4 and 10 for the gp61 data and a better fit of the peak of the response for the NP309 data. Statistically, this can be tested with the partial $F$ test. Comparing the two fits to the gp61 data yields $F_{2,17} = 17.7$, $p < 10^{-4}$, i.e., the two additional parameters significantly improve the quality of the fit. Although the full model fits the NP309 better, the improvement of the fit to this data is not statistically significant ($F_{2,9} = 1.9$, $p < 0.2$).

To obtain the fits for the gp61 epitope, we enforced that the time of the peak, $T$, could not occur before day 8. The data strongly suggest that the peak occurs around day 9. When we allowed the time of the peak to be a free parameter, it was estimated to occur at $T = 7.5$ days (data not shown). Because of compensation for this shorter expansion period, we obtained a higher estimate for proliferation rate of $\rho = 1.7\ d^{-1}$ (instead of the $\rho = 1.47\ d^{-1}$ with $T = 8$ days). Fitting the NP309 data without constraining the time of the peak, we obtained a realistic late peak around day 9 and a proliferation rate of $\rho = 1.11\ d^{-1}$. To test whether this difference in the estimated proliferation rates was real or was caused by the different times of the peak, we fitted the first five data points by linear regression. This confirmed the $\rho_{gp61} = 1.47\ d^{-1}$ and the $\rho_{NP309} = 1.11\ d^{-1}$ estimates of the proliferation rates and suggests that the immudominant clone proliferates 1.3-fold faster than the subdominant clone.

Since the $CD4^+$ T cell responses to the gp61 and NP309 LCMV epitopes probably have several parameters in common, we next fitted the two data sets simultaneously. To resolve the uncertainties about estimating the time of the peak, we fixed the proliferation rates to the values estimated above and again enforced that the time of the peak for the gp61 epitope could not occur before day 8 (Table II). Fitting the data simultaneously under these assumptions allows for fits that visually seems as good (Fig. 2) as those obtained with the individual fits with the biphasic model in Fig. 1. Comparing the fits of the full model with that of the model with a monophasic contraction phase, we find that the full model fits significantly better $F_{2,33} = 39.5$, $p < 10^{-6}$ with 42 data points fitted with nine versus seven parameters).

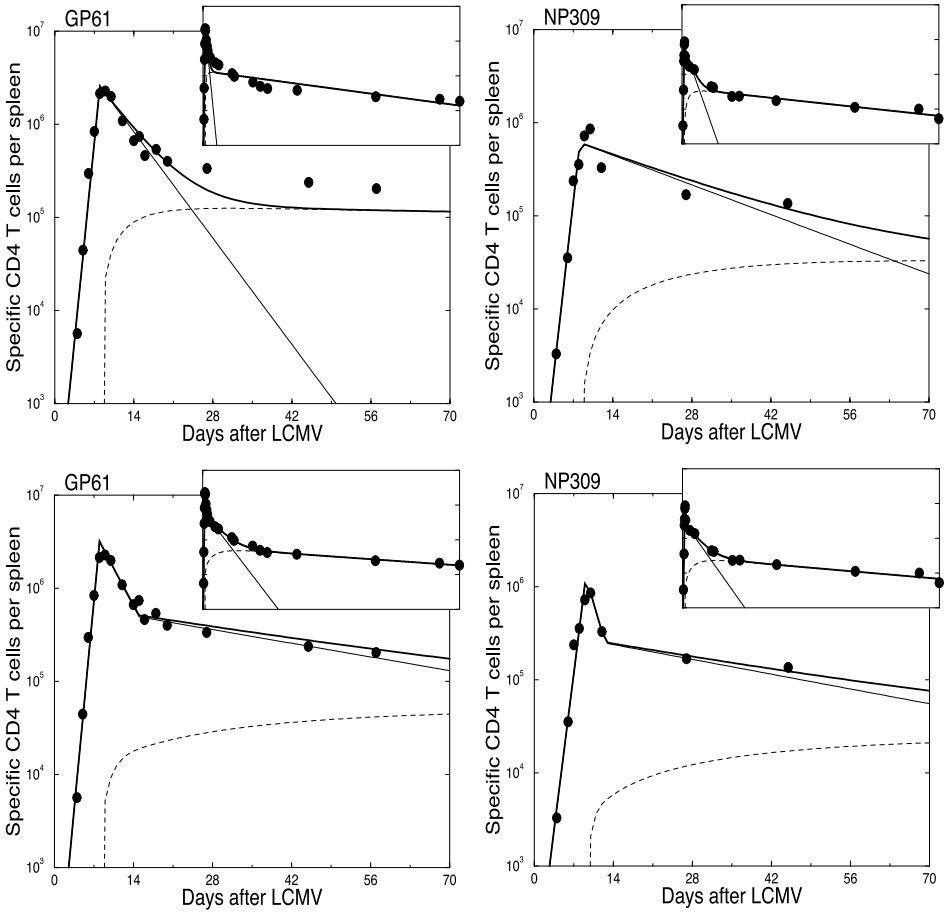


**FIGURE 1.** Fitting the dominant gp61 and the subdominant NP309 $CD4^+$ T cell responses individually. Dashed lines, Memory cells *M*; solid lines, activated cells *A*, heavy solid lines, totals $M + A$. *Top*, Model with one contraction phase (i.e., $\Delta = \alpha = 0$). *Bottom*, Model with biphasic contraction phase (i.e., $\Delta > 0$ and $\alpha > 0$). *Insets*, The same data for the entire time series of 921 days. See Table I for parameter estimates.

The two $CD4^+$ T cell responses differ in the proliferation rate $\rho$, which is higher for the dominant clone, in the generalized recruitment parameter $A(0)$, which is lower in the dominant clone and in the time of the peak *T*. The latter is an artifact due to the simplicity of the mathematical model which can only have a sharp peak value, whereas the $CD4^+$ T cell data clearly suggest a more rounded peak (Fig. 2). Measuring functional avidity by determining the fraction of specific IFN-$\gamma$-producing cells in peptide dilution assays, it was estimated that the avidity of gp61-specific $CD4^+$ T cells is almost 10-fold higher than $CD4^+$ T cells specific for NP309 (D. Homann, unpublished data). Such differences in avidity of the T cells for the peptide MHC (pMHC) complexes could influence the proliferation rate of the activated cells. The fact that the subdominant clone has the highest estimate for the generalized recruitment parameter means either that the naive precursor frequency of the NP309 response is higher and/or that naive

Table I. *Fitting the two $CD4^+$ T cell responses individually*[a]

| | | gp61 $CD4^+$ T Cells | | NP309 $CD4^+$ T Cells | |
|---|---|---|---|---|---|
| Name | Units | Value | 95% CI[b] | Value | 95% CI |
| $\rho$ | $d^{-1}$ | 1.40 | 1.23–1.59 | 1.24 | 1.07–1.39 |
| $\delta_A$ | $d^{-1}$ | 0.18 | 0.12–0.25 | 0.05 | 0.03–0.07 |
| $\delta_M$ | $d^{-1}$ | 0.0025 | 0.0018–0.0031 | 0.0020 | 0.0013–0.0026 |
| $r$ | $d^{-1}$ | 0.010 | 0.006–0.015 | 0.003 | 0.002–0.006 |
| $T$ | Days | 8 | 8–8 | 8.2 | 8–8.6 |
| $A(0)$ | Cells | 34.4 | 9.6–108.9 | 24.9 | 9.3–77.6 |
| $\rho$ | $d^{-1}$ | 1.47 | 1.37–1.58 | 1.11 | 0.96–1.25 |
| $\delta_A$ | $d^{-1}$ | 0.02 | 0.02–0.03 | 0.02 | 0.01–0.04 |
| $\delta_M$ | $d^{-1}$ | 0.0013 | 0.0006–0.0018 | 0.0016 | 0.0006–0.0022 |
| $r$ | $d^{-1}$ | 0.002 | 0.001–0.003 | 0.002 | 0.001–0.004 |
| $\alpha$ | $d^{-1}$ | 0.20 | 0.14–0.32 | 0.46 | 0.12–0.82 |
| $T$ | Days | 8 | 8–8 | 9.2 | 8.6–9.7 |
| $\Delta$ | Days | 7.0 | 5.1–9.0 | 3.4 | 2.2–9.4 |
| $A(0)$ | Cells | 24.0 | 11.3–47.2 | 49.4 | 22.7–151.4 |

[a] See Fig. 1 for a graphical representation. The gp61 and NP309 data sets contain 25 and 17 data points, respectively, and are fitted with either a six (*top*)- or an eight (*bottom*)-parameter model. The quality of the gp61 fits are MNSQ = 0.17 (six parameters) and MNSQ = 0.06 (eight parameters), respectively. The partial *F* test ($F_{2,17} = 17.7$, $p < 10^{-4}$) confirms that the eight-parameter model fits significantly better. The two fits of the NP309 data are more similar, i.e., MNSQ = 0.12 (six parameters) and MNSQ = 0.10 (eight parameters), respectively, with $F_{2,9} = 1.9$, $p < 0.2$.

[b] CI, Confidence interval.

Table II. *Fitting the two CD4$^+$ T cell responses simultaneously to a model with a rapid apoptosis window*[a]

| Name | Units | CD4$^+$ T Cells | |
|---|---|---|---|
| | | Value | 95% CI[b] |
| $\rho_{gp61}$ | $d^{-1}$ | 1.47 | — |
| $\rho_{NP309}$ | $d^{-1}$ | 1.11 | — |
| $\delta_A$ | $d^{-1}$ | 0.02 | 0.01–0.03 |
| $\delta_M$ | $d^{-1}$ | 0.0014 | 0.0007–0.0019 |
| $r$ | $d^{-1}$ | 0.002 | 0.001–0.003 |
| $\alpha$ | $d^{-1}$ | 0.21 | 0.16–0.28 |
| $T_{gp61}$ | Days | 8 | 8–8 |
| $T_{NP309}$ | Days | 8.8 | 8.6–9.1 |
| $\Delta$ | Days | 7.8 | 5.5–9.8 |
| $A(0)_{gp61}$ | Cells | 22.0 | 19.0–26.6 |
| $A(0)_{NP309}$ | Cells | 56.4 | 46.0–73.8 |

[a] See Fig. 2 for a graphical representation. By the partial $F$ test this fit with 10 parameters is significantly better than that obtained with $\Delta = \alpha = 0$ ($F_{2,33} = 30.7$, $p < 10^{-6}$). Because the subdominant clones have a better recruitment, the immunodominance is due to the faster proliferation of the gp61-specific response.

[b] CI, Confidence interval.

NP309-specific CD4$^+$ T cells are activated earlier than those of the dominant gp61 response. The latter could be due to an earlier expression of the NP309 epitope and/or higher pMHC concentrations (15).

To investigate whether the difference in immunodominance can also be explained with equal proliferation rates and a difference in recruitment only, we also fitted these data with three other models (data not shown). The first model has 11 free parameters and allows for different proliferation rates and different recruitment rates. The second and third models have 10 free parameters because we enforced equal recruitment rates and equal proliferation rates, respectively. In terms of the MNSQ distances, the best of the three is the one with different proliferation rates and equal recruitment. Moreover, by the $F$ test it is a significant improvement to expand the third model with an additional parameter allowing for different proliferation rates, i.e., comparing the first model with the third yields $F_{1,31} = 2.67$, $p < 0.001$. This suggests that the difference in immunodominance can best be explained with a difference in the proliferation rates. Since the precise value of the proliferation rate depends on the uncertain estimate of the time of the peak, we have most confidence in the $\rho_{gp61} = 1.47\ d^{-1}$ and the $\rho_{NP309} = 1.11\ d^{-1}$ estimates that we could confirm with linear regression on the first five data points (see above).

To characterize the specific CD4$^+$ T cell responses to LCMV kinetically, we translate the rates in Table II into doubling times and half-lives (Fig. 3*a*). During the expansion phase, the doubling time of the gp61 response is about 11 h and that of the NP309 response is about 15 h. The peak of the NP309 response is estimated to occur around day 9, that of the gp61 response is too rounded to be estimated with this model, but from the data appears to occur around the same time. During the initial rapid apoptosis phase that lasts another 8 days, the cells have a half-life of about 3 days. For activated cells, this increases to about 35 days after day 16. The memory cells have an estimated half-life of about 500 days (1.3 years). Following the peak, we estimate that on a daily basis 0.2% of the activated cells obtain the long-lived memory phenotype. Because activated cells are relatively long-lived, the build up of the memory population continues long after the peak of the response (Fig. 2). In the *Appendix*, we discuss a number of alternative fits to the CD4$^+$ T cell data and show that the poor estimate of the time of the peak does not affect the other results presented here.

### *CD8$^+$ T cells*

The total number of gp33-, NP396-, gp118-, gp276-, NP205-, and gp92-specific CD8$^+$ T cells in the spleen of the C57BL/6 mice can also be accurately described by the model (Fig. 4). Fitting the individual data sets for the CD8$^+$ T cell epitopes, we never found that allowing for a biphasic contraction phase gave a significant improvement of the fit. For most epitopes the simpler monophasic contraction model gave a better fit (i.e., had a lower MNSQ). Fitting the six CD8 data sets simultaneously allowed for very reasonable fits when we allowed the naive recruitment, $A(0)$, and the proliferation rate, $\rho$, to vary between the six epitopes (Table III). Allowing the net death rate of memory cells, $\delta_M$, to be a free parameter failed to improve the quality of the fit above that obtained when we fixed $\delta_M = 0$. This implies that the life time of CD8$^+$ T cell memory is sufficiently long that no significant decay could be observed in this data set extending over 921 days, i.e., in the mouse CD8$^+$ T cell memory seems to be lifelong.

The CD8$^+$ T cell responses to all six epitopes switch off around day 8. According to the peak response size, the dominance ranking of the six responses is gp33 > NP396 > gp118 > gp276 > NP205 > gp92. The parameter estimates in Table III suggest that the proliferation rate of the last two responses is significantly lower than that of the other four. The doubling time of the top four responses is about 8 h, that of the NP205 response 11 h, and that of the smallest gp92 response is 15 h. Differences in immunodominance are therefore partly due to differences in cellular proliferation rates during the expansion phase. It is surprising that these two subdominant clones have the largest estimates for the recruitment parameter (Table IV). One possible interpretation is that the NP205 and NP92 responses are actually composed of several clones all responding rather poorly but being present in relatively large numbers. The difference in immunodominance between the top four responses is largely due to differences in the generalized recruitment of precursor cells. Their estimated proliferation rates are very similar, and the rankings of their $A(0)$ parameters correspond perfectly with the observed immunodominance ranking. Again, differences in the naive recruitment parameter could reflect

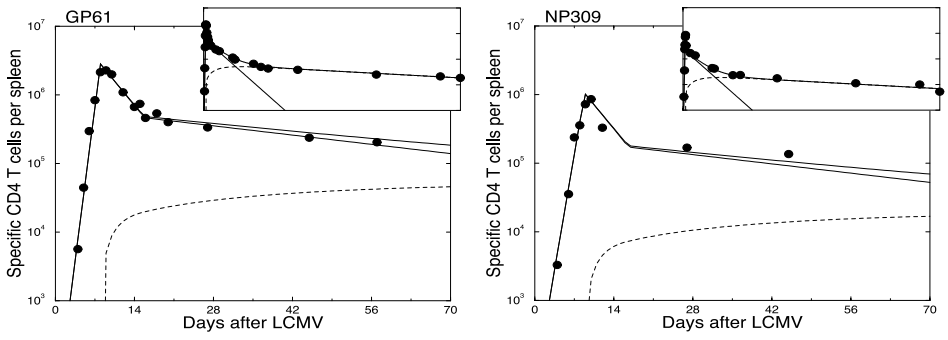


**FIGURE 2.** Fitting the dominant gp61 and the subdominant NP309 CD4$^+$ T cell responses simultaneously to a model with a biphasic contraction phase (i.e., $\Delta > 0$ and $\alpha > 0$). See Table II for parameter estimates.

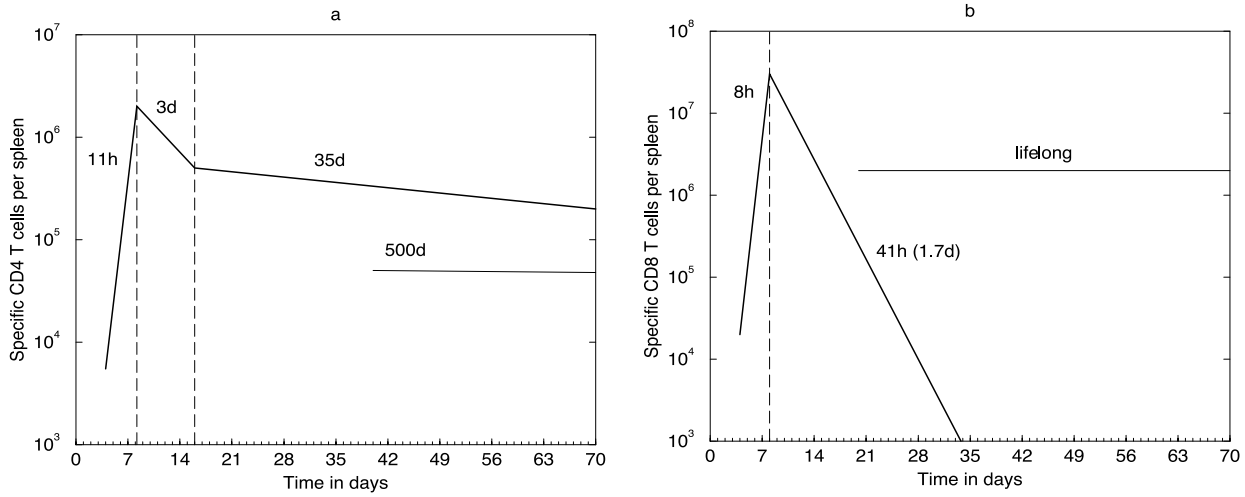


**FIGURE 3.** Schematic presentation of the immunodominant $CD4^+$ (*a*) and $CD8^+$ (*b*) T cell response to LCMV. The estimated doubling times and half-lives are indicated in each panel. The horizontal lines depict the memory phase: the half-life of $CD4^+$ memory is about 500 days, whereas that of the $CD8^+$ seems lifelong.

different precursor frequencies or earlier expression of the dominant epitopes, higher pMHC concentrations, and/or higher avidity (15). To explain the large differences between the six $CD8^+$ T cell responses, only small differences in their parameter values are required (Table III).

The immunodominant $CD8^+$ T cell response is characterized kinetically in Fig. 3*b*. During the expansion phase of 8 days, the doubling time is 8 h. We failed to find evidence for a biphasic contraction phase and estimate a half-life of 41 h for activated cells after the peak of the response. In addition, the memory phase of the $CD8^+$ T cell response is stable, with little evidence of memory decay.

### *Comparing $CD4^+$ and $CD8^+$ T cell dynamics*

The differences between the parameters characterizing the $CD4^+$ and $CD8^+$ T cell responses are striking (Fig. 3). $CD8^+$ T cell responses are faster in almost every aspect of the response. During the expansion phase, the doubling time of immunodominant $CD8^+$ T cells is approximately three-fourths of that of immunodominant $CD4^+$ T cells (i.e., 8 h vs 11 h). The rapid contraction phase of $CD4^+$ T cell responses lasts only 8 days, with a half-life of activated cells of 3 days. The corresponding half-life of activated $CD8^+$ T cells is 41 h (or 1.7 days). Moreover, activated $CD4^+$ T cells approach an even longer half-life of 35 days during the second half of the contraction phase. We failed to find evidence for such an increase in the half-life of activated $CD8^+$ T cells. The rate at which activated $CD8^+$ T cells become memory cells is also 10-fold faster than that of $CD4^+$ T cells. Because activated $CD4^+$ T cells live much longer than activated $CD8^+$ T cells (Fig. 3), the total number of memory cells that are formed after a $CD4^+$ T cell response need not be smaller than after a $CD8^+$ T cell response.

At day 70 of the gp61 $CD4^+$ T cell response, the estimated memory population size approaches its maximum value of $5 \times 10^4$ cells, which is 1.6% of the peak population size at day 8. At day 70 of the gp33 $CD8^+$ T cell response, we estimate a memory population of $1.4 \times 10^6$ cells (Fig. 4), which is 4% of the peak population size. The only phase that seems more dynamic in the $CD4^+$ T cell compartment is the memory phase. The half-life of $CD4^+$ T cell memory is about 500 days, whereas $CD8^+$ T cell memory seems not to decay. A long-lived memory need not be due to long-lived memory cells. It is well established that T cells with a memory phenotype divide more frequently than those with a naive phenotype (23–25). Thus, the fact that the $CD8^+$ T cell memory lasts longer than that of $CD4^+$ T cells could also be due to faster renewal kinetics of the $CD8^+$ memory T cells.

Finally, it seemed that the $CD4^+$ T cell responses shut off 1 day later than the CD8 responses (7). The data points shown in Figs. 1 and 2, which are averages of three to four mice, suggest that the $CD4^+$ T cells peak around days 9 and 10 for gp61 and NP309, respectively. However, there is scatter in the data and the SDs of the averages at days 9 and 10 are overlapping (data not shown), suggesting that the peak differs among mice and is not precisely defined. Because our model assumes that the response shuts off at a fixed time, *T*, it exhibits a sharp peak when the expansion phase ends, whereas the data have a more rounded peak. Thus, our current estimates for the time of the peak of the $CD4^+$ T cell response remain somewhat ambiguous. A model with a more rounded peak may yield a more reliable estimate for the precise time of the peak.

## Discussion

Homann et al. (7) suggested that in C57BL/6 mice the half-lives of the $CD4^+$ T cell populations involved in the primary immune response during acute LCMV Armstrong infection were increasing over time in several distinct phases after the peak of the response. Fitting a mathematical model to more detailed data from similar experiments, we have been able to confirm that the contraction phase of the $CD4^+$ T cell responses to gp61 and NP309 is biphasic, with an early half-life of 3 days and a late half-life of 35 days (Fig. 3*a*). In agreement with Homann et al. (7), we find that the $CD8^+$ T cell responses to six epitopes are better described with a monophasic contraction phase. However, the decline in the total number of specific $CD8^+$ T cells after the peak of the response slows down with time, i.e., at the total population level one does observe an increase in the half-life with time. The results of our model, depicted in Fig. 4, suggest that this is due to a gradual transition of short-lived activated cells into long-lived memory cells. Thus, although the average half-life of the population as a whole increases with time, those of the activated and memory subpopulation remain time invariant (see *Appendix*).

We previously estimated proliferation and death rates of the NP118 and gp283 $CD8^+$ T cell responses to $2 \times 10^5$ PFU of LCMV Armstrong injected i.p. into BALB/c mice (15). The estimates for the apoptosis rate $\delta_A$ and the rate $r$ at which cells adopt the memory phenotype were very similar to those estimated in

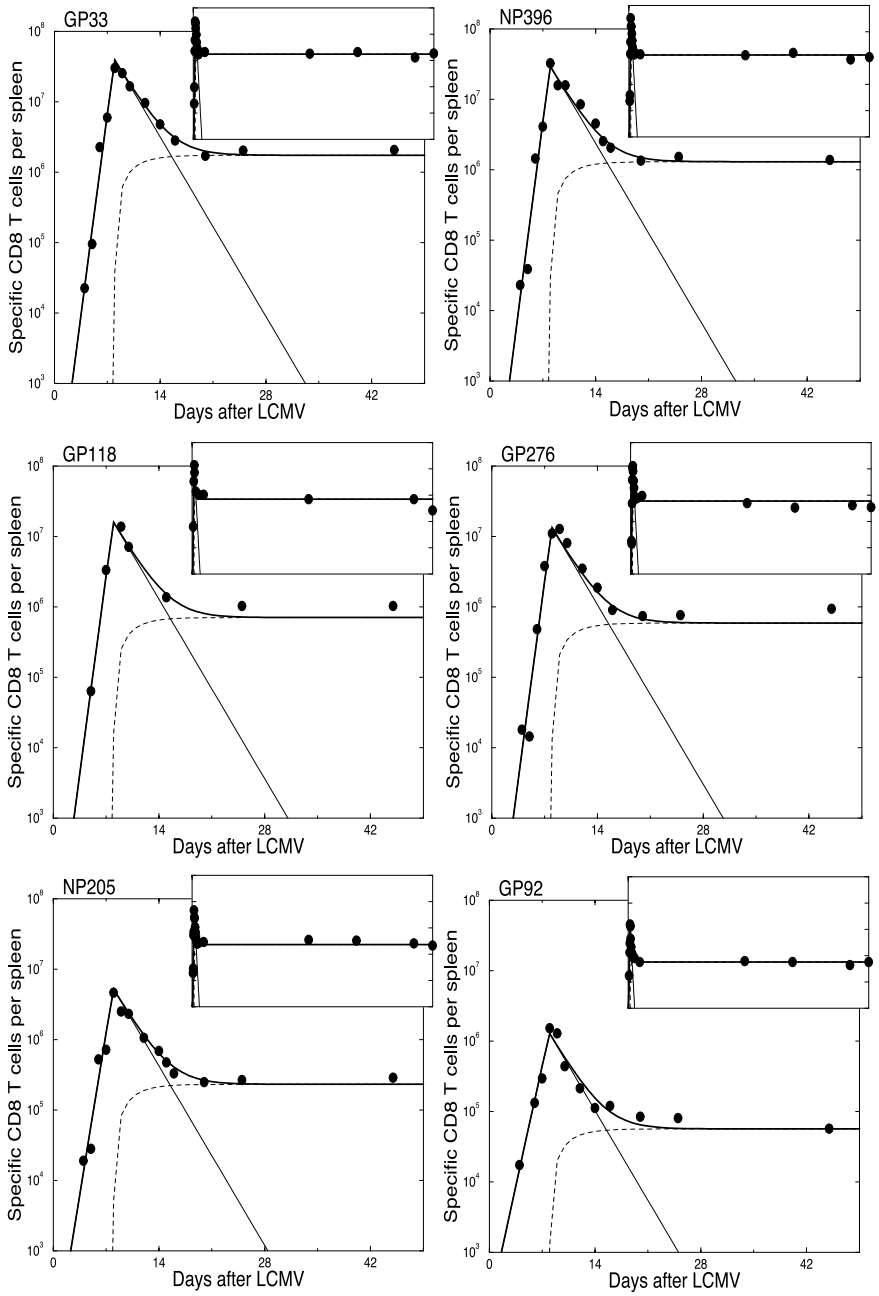


**FIGURE 4.** The $CD8^+$ T cell responses to six LCMV epitopes. The solid lines represent the best-fit model using the parameters in Table III. In the fits both the recruitment and the proliferation rates were allowed between the six epitopes. Data were fitted with the monophasic model, i.e., with $\Delta = \alpha = 0$.

Table III. In BALB/c mice the time of the peak was estimated to occur around day 6 however, and the proliferation rate was 2.8 $d^{-1}$. The estimates provided here for the $CD8^+$ T cell response to LCMV Armstrong epitopes in C57BL/6 mice are somewhat slower, i.e., the time of the peak is at day 8, and the proliferation rate is 1.9 $d^{-1}$ for the immunodominant $CD8^+$ responses. Apparently, BALB/c mice respond more vigorously, i.e., with faster cell division, to LCMV Armstrong than C57BL/6 mice do. Possibly as a consequence, their T cells stop proliferating earlier than those of C57BL/6 mice.

During vigorous primary immune reactions, both $CD4^+$ and $CD8^+$ T cell responses seem programmed to undergo clonal expansion in the absence of restimulation by Ag, followed by a contraction phase that also seems independent of antigen (9–14). The modeling of the data reported here suggests that $CD4^+$ and $CD8^+$ responses proceed through these phases fairly synchronously. We have shown that $CD4^+$ and $CD8^+$ T cells differ largely in the kinetics within each phase of an otherwise fairly similar program. The main qualitative difference that we found is the biphasic contraction of $CD4^+$ T cell responses. These results seem to be in disagreement with those of Foulds et al. (14) who compared $CD4^+$ and $CD8^+$ T cell responses during *Listeria* infection. They found that $CD4^+$ T cells divide a limited number of times in contrast to $CD8^+$ T cells, which undergo more extensive clonal expansion. Since these differences remained when $CD4^+$ and $CD8^+$ T cells were uniformly stimulated with anti-CD3 mAb, they suggested that $CD4^+$ and $CD8^+$ T cells have different programs for the expansion phase (14). The modeling of our data has provided an additional insight in the differences between $CD4^+$ and $CD8^+$ T cell responses. In our interpretation, $CD4^+$ and $CD8^+$ T cells follow similar programs, switching off expansion at similar or possibly somewhat later times for $CD4^+$ T cells. However, $CD4^+$ T cells divide slower, with a 1.4-fold longer doubling time, which implies that $CD4^+$ T cells complete three-fourths of the divisions completed by $CD8^+$ T cells during the same time period, which is consistent with the observation of Foulds et al. (14) for the response to *Listeria.*

Table III. *Parameter estimates obtained by fitting the CD8$^+$ T cell response with proliferation and recruitment parameters different for each of the six epitopes*[a]

| Name | Units | Value | 95% CI[b] |
|---|---|---|---|
| $\rho_{gp33}$ | $d^{-1}$ | 1.89 | 1.73–2.08 |
| $\rho_{NP396}$ | $d^{-1}$ | 1.92 | 1.75–2.14 |
| $\rho_{gp118}$ | $d^{-1}$ | 1.86 | 1.60–2.21 |
| $\rho_{gp276}$ | $d^{-1}$ | 1.87 | 1.70–2.05 |
| $\rho_{NP205}$ | $d^{-1}$ | 1.52 | 1.37–1.69 |
| $\rho_{gp92}$ | $d^{-1}$ | 1.13 | 0.98–1.33 |
| $A(0)_{gp33}$ | Cells | 12.1 | 3.3–32.5 |
| $A(0)_{NP396}$ | Cells | 6.9 | 1.3–20.7 |
| $A(0)_{gp118}$ | Cells | 6.1 | 0.4–40.3 |
| $A(0)_{gp276}$ | Cells | 5.0 | 1.3–13.9 |
| $A(0)_{NP205}$ | Cells | 29.3 | 8.6–81.9 |
| $A(0)_{gp92}$ | Cells | 165.3 | 34.4–518.8 |
| $\delta_A$ | $d^{-1}$ | 0.40 | 0.34–0.47 |
| $r$ | $d^{-1}$ | 0.018 | 0.015–0.022 |
| $T$ | Days | 7.9 | 7.8–8.1 |

[a] See Fig. 4 for a graphical representation. The results were obtained with the monophasic contraction model because the more complicated biphasic model failed to fit significantly better ($F_{2,79} = 0.84$, $p < 0.5$, with 96 data points and 17 vs 15 parameters). Also, fitting with $\delta_M \neq 0$ failed to improve the quality of the fit, so the death rate of memory cells was fixed at $\delta_M = 0$.

[b] CI, Confidence interval.

The peak of the CD8$^+$ T cell responses seems sharp, well-defined, and synchronous for all epitopes (Fig. 4). For CD4$^+$ T cells, the data not only suggest that the peak occurs about a day later, but also that it is more rounded. One possible mechanism for accounting for a more rounded peak would be that the onset of apoptosis precedes the switch off of proliferation. This would slow down the net rate of expansion and hence round the peak. To incorporate this difference in timing into the mathematical model, one can extend it with an additional parameter, $T_\alpha$, for the onset of apoptosis, whenever $T_\alpha < T$ the model will have a more rounded peak. Annexin V staining indeed suggests an increase in apoptosis before the peak of the response (D. Homann, unpublished data). However, it remains unclear whether this explains the rounded CD4$^+$ T cell peak because the fraction of annexin V$^+$ cells is more than 2-fold larger in the CD8$^+$ T cell compartment than it is in CD4$^+$ T cells around the peak of the response. The high annexin V expression in the CD8$^+$ T cell compartment is an independent confirmation of the high apoptosis rate that we have estimated for CD8$^+$ T cells (Fig. 3).

We have modeled the contraction phase of the CD4$^+$ T cells with two time windows with a different death rate of the activated cells in each. Such a model is purely phenomenological and provides no biological mechanism by which death rates change. One can speculate about mechanisms. For example, one possibility is that activated cells have a fast death rate, $\delta_A + \alpha$, directly after the peak, and that they are rescued from apoptosis, say by activation of BCL2, at a rate $r'$ to become activated cells with a death rate $\delta_A$. With this model, one obtains a gradual transition between the two windows in the contraction phase rather than the sharp transition depicted in Fig. 2. The equations for this alternative model are given in the *Appendix*. Another possibility is that the population at the time of the peak is heterogeneous. A certain fraction $f$ could be apoptotic and have a fast death rate, while the other fraction $(1 - f)$ decays more slowly and slowly attains the memory phenotype. The equations are in the *Appendix*. Both alternative models, and probably many more, have a behavior that is very similar to that of the more phenomenological model considered here (data not shown). We have analyzed these two alternative models and have obtained parameter estimates for the rescue rate, $r' = 0.06\ d^{-1}$ (Table IV), and for the fraction of apoptotic cells, $f = 0.82$ (Table IV), giving fits to the CD4$^+$ T cell data that seem indistinguishable from those in Fig. 2 (data not shown). Thus, the parameter estimates for the length of the apoptosis window, $\Delta$, and the additional death rate of the apoptotic cells, $\alpha$, depend on the assumptions of our phenomenological model. Fortunately, the other parameter estimates remain similar when we fitted the two alternative models to the data, and hence appear to be robust (Table IV).

Earlier articles studying the TCR repertoire of CD8$^+$ T cell responses to the LCMV epitopes demonstrate that each response is composed of a number of different clones (26, 27). The parameter estimates provided in this article should therefore be interpreted as averages over all clones participating in the response to each particular epitope. The high estimate of the recruitment parameter of the two subdominant NP205 and NP92 CD8$^+$ T cell responses could indeed reflect that these responses are relatively broad and that they start with a relatively high number of precursor cells. In agreement with earlier articles, we find that the recruitment of precursor cells is a major factor determining immunodominance (4, 28, 29). We extend this by demonstrating that the proliferation rate during the expansion phase seems an equally important factor.

## Appendix

The model defined by Equations 1–3 is piecewise linear. When $t \leq T$ activated cells expand exponentially at a rate $\rho$ such that the solution obeys

$$A(t) = A(0)\exp[\rho t];\ M(t) = 0. \quad (4)$$

Table IV. *Parameter estimates of the two alternative models in the Appendix*

| | | Rescue: Equation 9 | | Fraction: Equation 10 | |
|---|---|---|---|---|---|
| Name | Units | Value | 95% CI[a] | Value | 95% CI |
| $\rho_{gp61}$ | $d^{-1}$ | 1.47 | — | 1.47 | — |
| $\rho_{NP309}$ | $d^{-1}$ | 1.11 | — | 1.11 | — |
| $\delta_A + \alpha$ | $d^{-1}$ | 0.38 | 0.26–0.57 | 0.40 | 0.29–0.58 |
| $\delta_A$ | $d^{-1}$ | 0.019 | 0.013–0.026 | 0.019 | 0.013–0.026 |
| $\delta_M$ | $d^{-1}$ | 0.0014 | 0.0007–0.0018 | 0.0013 | 0.0007–0.0018 |
| $r'$ | $d^{-1}$ | 0.063 | 0.036–0.011 | | |
| $r$ | $d^{-1}$ | 0.003 | 0.001–0.005 | 0.002 | 0.001–0.004 |
| $T_{gp61}$ | Days | 8 | 8–8 | 8 | 8–8 |
| $T_{NP309}$ | Days | 9.1 | 8.8–9.3 | 8.9 | 8.7–9.2 |
| $A(0)_{gp61}$ | Cells | 24.1 | 20.3–29.9 | 22.9 | 19.7–27.4 |
| $A(0)_{NP309}$ | Cells | 50.3 | 41.3–63.6 | 56.6 | 45.0–70.4 |
| $f$ | — | | | 0.82 | 0.75–0.87 |

[a] CI, Confidence interval.

Following the peak, i.e., for $T \leq t \leq T + \Delta$, the solutions of Equations 2 and 3 obey

$$A(t) = A(T)\exp[-\delta(t - T)], \quad (5)$$

$$M(t) = \frac{\exp[-\delta_M t](rA(T)(1 - \exp[-(\delta - \delta_M)t]))}{\delta - \delta_M}, \quad (6)$$

where $\delta = r + \delta_A + \alpha$ and $A(T)$ is given by Equation 4. When $t > T + \Delta$ the solution is

$$A(t) = A(T + \Delta)\exp[-\delta'(t - T - \Delta)], \quad (7)$$

$$M(t) = \frac{\exp[-\delta_M t](rA(T + \Delta)(1 - \exp[-(\delta' - \delta_M)t]) + M(T + \Delta)(\delta' - \delta_M)}{\delta' - \delta_M}, \quad (8)$$

where $\delta' = r + \delta_A$ and $A(T + \Delta)$ is given by Equation 5 and $M(T + \Delta)$ is given by Equation 6.

The $CD8^+$ T cell data were fitted with the $\Delta = \alpha = 0$ model because 1) the data and the fits displayed in Fig. 4 suggest that the decline of activated $CD8^+$ T cells is monophasic and 2) the $F$ test suggested that the more complicated biphasic contraction model failed to fit the data better than the simpler model (see footnote to Table III). Surprisingly, the biphasic contraction model allowed for an alternative interpretation of the data. Fitting the $CD8^+$ T cell data to this model, we obtained parameter estimates of an apoptosis window $\Delta = 8.5$ days, no reversal to memory ($r \simeq 0$) and a very long half-life of activated cells. Mathematically, this is a natural result: activated cells die rapidly during the first 8.5 days after the peak of the response and obtain a long half-life afterward, i.e., if the activated cells take over the role of the long-lived memory cells, all cells would synchronously obtain a long life span after $T + \Delta$ days. Although one can describe the data following the peak with such a biphasic decline of a single population, we prefer the biologically more realistic model in which short-lived activated cells slowly become long-lived memory cells. Thus, the $F$ test reported in the text was for a model in which we enforced formation of memory cells by requiring $r > 0.01$.

One could argue that we should also have modeled the apoptosis window of length $\Delta$ with two subpopulations of activated cells. A first possibility is the following model for time after the peak, i.e., for $t > T$,

$$\frac{dA_0}{dt} = -(\alpha + \delta_A + r')A_0, \frac{dA_1}{dt} = r'A_0 - (\delta_A + r)A_1 \text{ and}$$

$$\frac{dM}{dt} = rA_1 - \delta_M M, \quad (9)$$

with the initial condition $A_0(T) = A(T)$ and $A_1(T) = M(T) = 0$. The time window parameter $\Delta$ has been replaced by a rate $r'$ at which apoptotic cells become rescued. We have fitted the solutions of this model to the $CD4^+$ cell data (Table IV).

An alternative model is that one starts with an apoptotic subpopulation $A_0$ and a nonapoptotic subpopulation $A_1$ at the time of the peak:

$$\frac{dA_0}{dt} = -(\alpha + \delta_A)A_0, \frac{dA_1}{dt} = -(\delta_A + r)A_1 \text{ and } \frac{dM}{dt} = rA_1 - \delta_M M, \quad (10)$$

with the initial condition $A_0(T) = fA(T)$, $A_1(T) = (1 - f)A(T)$, and $M(T) = 0$. We have also fitted the solutions of this model to the $CD4^+$ T cell data (Table IV).

## References


1. Lau, L. L., B. D. Jamieson, T. Somasundaram, and R. Ahmed. 1994. Cytotoxic T-cell memory without antigen. *Nature 369:648.*
2. Asano, M. S., and R. Ahmed. 1996. CD8 T cell memory in B cell-deficient mice. *J. Exp. Med. 183:2165.*
3. Zimmerman, C., K. Brduscha-Riem, C. Blaser, R. M. Zinkernagel, and H. Pircher. 1996. Visualization, characterization, and turnover of $CD8^+$ memory T cells in virus-infected hosts. *J. Exp. Med. 183:1367.*
4. Murali-Krishna, K., J. D. Altman, M. Suresh, D. J. Sourdive, A. J. Zajac, J. D. Miller, J. Slansky, and R. Ahmed. 1998. Counting antigen-specific CD8 T cells: a reevaluation of bystander activation during viral infection. *Immunity 8:177.*
5. Butz, E. A., and M. J. Bevan. 1998. Massive expansion of antigen-specific $CD8^+$ T cells during an acute virus infection. *Immunity 8:167.*
6. Ahmed, R., and D. Gray. 1996. Immunological memory and protective immunity: understanding their relation. *Science 272:54.*
7. Homann, D., L. Teyton, and M. B. Oldstone. 2001. Differential regulation of antiviral T-cell immunity results in stable $CD8^+$ but declining $CD4^+$ T-cell memory. *Nat. Med. 7:913.*
8. Mercado, R., S. Vijh, S. E. Allen, K. Kerksiek, I. M. Pilip, and E. G. Pamer. 2000. Early programming of T cell populations responding to bacterial infection. *J. Immunol. 165:6833.*
9. Van Stipdonk, M. J., E. E. Lemmens, and S. P. Schoenberger. 2001. Naive CTLs require a single brief period of antigenic stimulation for clonal expansion and differentiation. *Nat. Immunol. 2:423.*
10. Kaech, S. M., and R. Ahmed. 2001. Memory $CD8^+$ T cell differentiation: initial antigen encounter triggers a developmental program in naive cells. *Nat. Immunol. 2:415.*
11. Badovinac, V. P., B. B. Porter, and J. T. Harty. 2002. Programmed contraction of $CD8^+$ T cells after infection. *Nat. Immunol. 3:619.*
12. Bajenoff, M., O. Wurtz, and S. Guerder. 2002. Repeated antigen exposure is necessary for the differentiation, but not the initial proliferation, of naive $CD4^+$ T cells. *J. Immunol. 168:1723.*
13. Lee, W. T., G. Pasos, L. Cecchini, and J. N. Mittler. 2002. Continued antigen stimulation is not required during $CD4^+$ T cell clonal expansion. *J. Immunol. 168:1682.*
14. Foulds, K. E., L. A. Zenewicz, D. J. Shedlock, J. Jiang, A. E. Troy, and H. Shen. 2002. Cutting edge: CD4 and CD8 T cells are intrinsically different in their proliferative responses. *J. Immunol. 168:1528.*
15. De Boer, R. J., M. Oprea, R. Antia, K. Murali-Krishna, R. Ahmed, and A. S. Perelson. 2001. Recruitment times, proliferation, and apoptosis rates during the $CD8^+$ T-cell response to lymphocytic choriomeningitis virus. *J. Virol. 75:10663.*
16. Ciurea, A., P. Klenerman, L. Hunziker, E. Horvath, B. Odermatt, A. F. Ochsenbein, H. Hengartner, and R. M. Zinkernagel. 1999. Persistance of lymphocytic choriomeningitis virus at very low levels in immune mice. *Proc. Natl. Acad. Sci. USA 96:11964.*
17. Murali-Krishna, K., L. L. Lau, S. Sambhara, F. Lemonnier, J. Altman, and R. Ahmed. 1999. Persistence of memory CD8 T cells in MHC class I-deficient mice. *Science 286:1377.*
18. Blattman, J. N., R. Antia, D. J. Sourdive, X. Wang, S. M. Kaech, K. Murali-Krishna, J. D. Altman, and R. Ahmed. 2002. Estimating the precursor frequency of naive antigen-specific CD8 T cells. *J. Exp. Med. 195:657.*
19. Stetson, D. B., M. Mohrs, V. Mallet-Designe, L. Teyton, and R. M. Locksley. 2002. Rapid expansion and IL-4 expression by *Leishmania*-specific naive helper T cells in vivo. *Immunity 17:191.*
20. Marquardt, D. W. 1963. Finite difference algorithm for curve fitting. *J. Soc. Ind. Appl. Math. 11:431.*
21. Efron, B., and R. Tibshirani. 1986. Bootstrap methods for standard errors, confidence intervals, and other measures of statistical accuracy. *Stat. Sci. 1:54.*
22. Armitage, P. and G. Berry. 1994. *Statistical Methods in Medical Research*, 2nd Ed. Blackwell, Oxford.
23. Michie, C. A., A. McLean, C. Alcock, and P. C. Beverley. 1992. Lifespan of human lymphocyte subsets defined by CD45 isoforms. *Nature 360:264.*
24. Clark, D. R., R. J. De Boer, K. C. Wolthers, and F. Miedema. 1999. T cell dynamics in HIV-1 infection. *Adv. Immunol. 73:301.*
25. De Boer, R. J., H. Mohri, D. D. Ho, and A. S. Perelson. 2003. Turnover rates of B cells, T cells, and NK cells in simian immunodeficiency virus-infected and uninfected rhesus macaques. *J. Immunol. 170:2479.*
26. Blattman, J. N., D. J. Sourdive, K. Murali-Krishna, R. Ahmed, and J. D. Altman. 2000. Evolution of the T cell repertoire during primary, memory, and recall responses to viral infection. *J. Immunol. 165:6081.*
27. Slifka, M. K., J. N. Blattman, D. J. Sourdive, F. Liu, D. L. Huffman, T. Wolfe, A. Hughes, M. B. Oldstone, R. Ahmed, and M. G. Von Herrath. 2003. Preferential escape of subdominant $CD8^+$ T cells during negative selection results in an altered antiviral T cell hierarchy. *J. Immunol. 170:1231.*
28. Bousso, P., J. P. Levraud, P. Kourilsky, and J. P. Abastado. 1999. The composition of a primary T cell response is largely determined by the timing of recruitment of individual T cell clones. *J. Exp. Med. 189:1591.*
29. Yewdell, J. W., and J. R. Bennink. 1999. Immunodominance in major histocompatibility complex class I-restricted T lymphocyte responses. *Annu. Rev. Immunol. 17:51.*